

***DX*-like properties of the *EL6* defect family in GaAs**

C. V. Reddy, Y. L. Luo, S. Fung, and C. D. Beling

Department of Physics, The University of Hong Kong, Pokfulam Road, Hong Kong, People's Republic of China

(Received 18 February 1998)

Capacitance-voltage characterization at different temperatures and emission and capture deep-level transient spectroscopy carried out on undoped *n*-type GaAs lend strong confirmation to the recent suggestion that the *EL6* defect arises from a center that is *DX*-like in nature. The evidence comes from the observation of an anomalous filling pulse duration dependence of the peak intensities of three to four different *EL6* sublevels, similar to that recently found for the *DX* center in $\text{Al}_x\text{Ga}_{1-x}\text{As}$ and attributed to the charge redistribution. In addition, capture transients reveal large capture barriers (0.2–0.3 eV), which are typical of a defect undergoing large lattice relaxation into a deep-lying state. These observations indicate that the *EL6* defect center comprises of a center with three to four slightly different ground-state configurations, each one of which forms as a result of some bond-breaking atomic displacement on capture of a second electron at the defect site. The significance of this in understanding the microstructure for the *EL6* center is briefly discussed.

[S0163-1829(98)00327-0]

I. INTRODUCTION

The deep levels *EL2*, *EL3*, and *EL6* are the three most commonly observed deep levels caused by native defects in bulk-grown, undoped GaAs.^{1–4} In general, *EL2* and *EL6* appear at larger concentrations, while *EL3* appears at lesser, sometimes even negligible, concentrations. Of all the native defects in GaAs, *EL2* has gained the most attention because of its interesting properties such as its metastability and its technological importance in producing material with semi-insulating (SI) character. The atomic structure of this defect is widely accepted as As_{Ga} with a possible interaction of As_i .⁵ However, it has been pointed out that in both the SI and “failed” SI GaAs material, medium deep donors, shallower than *EL2*, also play a significant role in determining the electrical behavior of these materials.⁶ In particular, temperature-dependent Hall and deep-level transient spectroscopy (DLTS) measurements have given direct evidence that *EL6* plays an important role in the decrease of the resistivity of undoped GaAs crystals.^{7–9}

The work of Chantre, Vincent, and Bois showed that the *EL6* defect possessed some interesting properties.¹⁰ In their experiment, it was found that *EL6* exhibited very different thermal (~ 0.3 eV) and optical ionization energies (~ 0.86 eV), suggesting a large lattice relaxation (LLR) effect for this defect. The lack of uniaxial stress effects on the symmetry¹¹ and the electron emission rate¹² of the *EL6* center is consistent with the above observation since stress effects would be absent for a defect with LLR with symmetry being maintained even under the application of stress. With LLR being the normally proposed mechanism to explain the persistent photoconductivity (PPC) phenomena, observed in many of the III-V and II-VI compound semiconductors, such as $\text{Al}_x\text{Ga}_{1-x}\text{As}$, $\text{In}_x\text{Ga}_{1-x}\text{As}$, and $\text{Cd}_x\text{Zn}_{1-x}\text{Te}$,¹³ the discovery of Chantre, Vincent, and Bois¹⁰ suggested that PPC might also be seen in GaAs. Experiments on GaAs have, however, aimed largely at studying photocurrent quenching (PCQ) rather than PPC, although the latter has often been observed

after PCQ and the subsequent onset of the enhancement of the photocurrent (EPC).^{14,15} While photoquenching is well understood in terms of the transformation of the *EL2* from its normal to the optically and electrically inactive metastable state *EL2**, the causes of the EPC and PPC effects are less well understood. Recently, however, Mitchel and Jiménez have convincingly argued that these effects result from the large lattice relaxation and associated low-temperature metastability of some other defect site, the most likely candidate of which is the *EL6* center.¹⁶

The negative-*U* ordering of the energy states of the *DX* center with increasing electron occupancy is an important characteristic feature in compound semiconductors such as $\text{Al}_x\text{Ga}_{1-x}\text{As}:\text{Si}$, which exhibit PPC.^{17,18} The defect state corresponding to the first electron occupancy is simply the shallow (Si_{Ga}) donor substitutional site, whereas the defect state with two-electron occupancy is deeper and is associated with a bond-breaking LLR. In such materials it is observed that the DLTS spectra display a multiple-peak structure for the two-electron occupancy (*DX*[−]) state, while for a single-electron occupancy state only a single peak is observed.^{19,20} While the sequential emission of two electrons to the conduction band would be expected to give a peak with twice the amplitude, there is no immediately apparent reason for the deep-level splitting. To explain this observation, a number of models such as small lattice relaxation²¹ and alloy disordering²² have been proposed. It is, however, the charge redistribution model, as proposed by Su and Farmer,^{23,24} within the framework of the broken bond model of Chadi and Chang,¹⁷ that most sensibly accounts for the observation of a multipeak structure. The aim of the present paper is to present data showing that the *EL6* defect in *n*-type GaAs has properties closely resembling the *DX* center in $\text{Al}_x\text{Ga}_{1-x}\text{As}:\text{Si}$. Not only is there the similar multilevel structure, but in addition the same charge redistribution is found between the sublevels during trap filling.^{23,24} Following the same reasoning of Su and Farmer, we argue that these observations give strong evidence for *EL6* being *DX*-like in nature.

This paper is structured as follows. Experimental details are given in Sec. II. In Sec. III the capacitance-voltage (C - V) measurements taken at different temperatures are presented first, these being required for the interpretation of the DLTS spectra. The charge redistribution phenomenon seen in the DLTS emission spectra taken at different trap filling times are then presented and here, as mentioned above, it is argued that these give the most convincing evidence that $EL6$ is DX -like in nature. In this section the possible charge states of the $EL6$ center are discussed. The last part of this section describes capture DLTS measurements of the electron capture barrier height for the $EL6$ center, which show a large capture barrier height for the defect that is consistent with the data and LLR proposition of Chantre, Vincent, and Bois.¹⁰ Finally, in Sec. IV some conclusions are drawn.

II. EXPERIMENT

The samples used in the present study were cut from a horizontal gradient freeze grown, undoped, n -type GaAs wafer, procured from MCP Wafer Technology Ltd., United Kingdom. The free carrier concentration was given as $\sim 10^{16} \text{ cm}^{-3}$. The samples were degreased and then given an acid etch in $\text{NH}_4\text{OH}:\text{H}_2\text{O}_2:\text{H}_2\text{O}$ (1:1:5) for 1 min followed by an etch in $\text{H}_2\text{SO}_4:\text{H}_2\text{O}_2:\text{H}_2\text{O}$ (10:1:1) for 1 min to remove the native oxide. After rinsing in deionized water and drying in dry nitrogen gas, a Sn Ohmic contact was made by alloying at 420°C . On the reverse side of the sample, so as to facilitate the DLTS measurements, Ag Schottky contacts of 1 mm diameter were made by thermal evaporation through a mask.

The C - V measurements were made in the standard way, using a Boonton capacitance meter. At each temperature the Schottky contact was reverse biased in steps of 0.1 V up to a maximum of 5 V, the total scan time being 500 s. The temperature was controlled to 0.1°C using an Oxford Instruments ITC4 controller.

The DLTS measurements were carried out using a home-built system capable of observing both capture and emission transients, the details of which have been published elsewhere.^{25,26} A standard DLTS activation analysis confirmed that there were two dominant deep levels in the material centered at 0.375 and 0.83 eV below the conduction band. These could easily be identified with the $EL6$ and $EL2$ levels, respectively, according to the Martin-Mitonneau-Mircea classification scheme.²⁷ Another defect with an activation energy of 0.62 eV, identified with $EL3$, was also observed, but at negligible concentration compared to that of $EL6$ and $EL2$. The DLTS measurements in the present experiment were recorded as a function of filling pulse duration (t_p), which was varied from 10 ns to the 1 s maximum permissible on our apparatus.

III. RESULTS AND DISCUSSION

A. C - V measurements

C - V scans were taken on our samples so as to gain some information of the concentration of various electron-trapping centers in the GaAs. In our C - V measurements the time scale of capacitance sampling (~ 10 s) is slow enough to allow some deep levels to emit, while others with longer emission

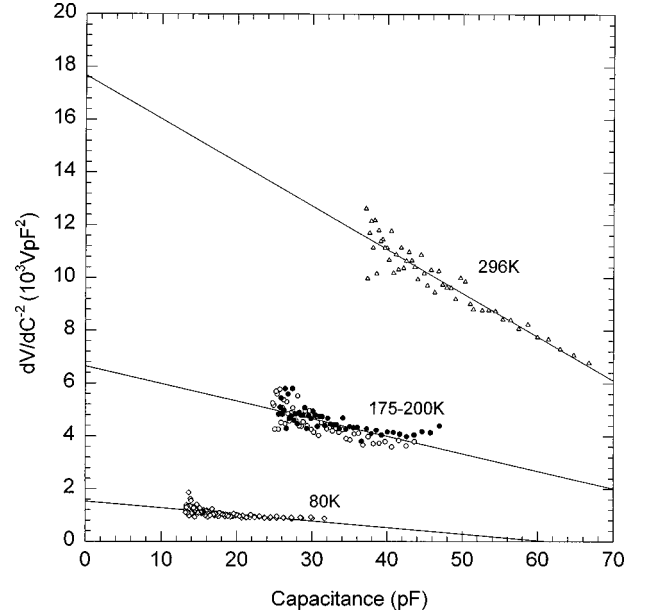


FIG. 1. Isothermal capacitance voltage measurements made on undoped n -type GaAs at 80 K (\diamond), 175 K (\circ), 200 K (\bullet), and 296 K (\triangle). The derivative of the reverse bias V with respect to $1/C^2$ is plotted against the capacitance C (as in Ref. 28) so as to separate the trap density N_T from the shallow donor density N_D .

times than this stay electron occupied. At a given temperature the traps with emission time less than ~ 10 s will change their occupation and follow the variation of the applied bias and thus their ionization will add to the depletion region charging already imposed by the shallow donor levels; this in turn increases the junction capacitance. Our sample was observed to undergo transitions in C - V characterization at around 150 and 250 K, which are associated with the ionization of the $EL6$ and $EL2$ levels, respectively.

With significant deep-level ionization in our sample it is no longer valid to perform a standard $1/C^2$ vs V plot to find the net donor density, but instead it is necessary to plot the inverse gradient $\partial V/\partial C^{-2}$ of that plot against C since from theory²⁸

$$\frac{\partial V}{\partial C^{-2}} = \frac{e\epsilon A^2}{2}(N_D + N_T) - \frac{\lambda N_T e A}{2} C, \quad (1)$$

where e is the electronic charge, ϵ is the material permittivity, A is the junction area, N_D is the density of shallow donors [defined as those donor levels that can ionize within a period ($\sim 10^{-6}$ s) of the test frequency of the capacitance meter], and N_T is the concentration of deep levels that emit within the rather broad time interval $\sim 10^{-6}$ –10 s. The distance λ in Eq. (1) is that distance beyond the free carrier tail over which the deep levels are still below the Fermi energy, and thus occupied, and is given by²⁹

$$\lambda = \left(\frac{2\epsilon(E_F - E_T)}{eN_D} \right)^{1/2}. \quad (2)$$

The plot of $\partial V/\partial C^{-2}$ plotted against C is shown in Fig. 1 for the temperatures 80, 175, 200, and 296 K. Straight lines are obtained for which we note, from Eqs. (1) and (2), that the intercept of the y axis gives $N_D + N_T$ and the gradient a value

TABLE I. Values of N_T and N_D as obtained from the fitting of Eq. (1) to the C - V data. The error on N_T is compounded from the uncertainty in the gradient and the estimated errors on the trap energy and Fermi-level positions. The asterisk means the designation is somewhat uncertain.

Temperature (K)	N_T+N_D from intercept (cm^{-3})	N_T from gradient (cm^{-3})	N_D (cm^{-3})	E_F-E_T (eV)
80	$8.5(0.3)\times 10^{14}$	$6.7(1.2)\times 10^{14}$	$1.8(1.2)\times 10^{14}$	0.15(0.05) due to $EL15^*$
175–200	$3.7(0.2)\times 10^{15}$	$2.7(0.5)\times 10^{15}$	$1.0(0.5)\times 10^{15}$	0.37(0.07) due to $EL6$
296	$9.9(0.3)\times 10^{15}$	$7.2(0.6)\times 10^{15}$	$2.7(0.7)\times 10^{15}$	0.8(0.1) due to $EL2$

of $N_T/N_D^{0.5}$, some suitable approximation being made for the trap energy E_F-E_T so as to form an estimate of λ through Eq. (2). We have in the present analysis approximated E_F as the conduction band and E_T as the ionization energy of the trap being ionized as determined by DLTS measurements. The former approximation is justified in view of the n -type conductivity of the sample. The data of Fig. 1 thus allow estimates of both N_T and N_D to be made. These are listed in Table I.

The C - V scans in the plateau region 175–200 K are essentially the same and reveal $EL6$ to be present at a concentration of $\sim 3\times 10^{15} \text{ cm}^{-3}$ (or $\sim 1.5\times 10^{15} \text{ cm}^{-3}$ if the center is a double donor). This ionization takes place against a background charge concentration N_D of $\sim (1.0\pm 0.5)\times 10^{15} \text{ cm}^{-3}$. This, as discussed below, turns out to be important since the usually employed DLTS approximation that $N_T \ll N_D$ does not apply and more care is required in the extraction of the defect concentration. The background N_D is also noted to be consistent with the expected amount of background ionization based upon the 80-K C - V data [$N_D+N_T = (0.85\pm 0.03)\times 10^{15} \text{ cm}^{-3}$], which appears to originate from both a shallow donor at the $2\times 10^{14} \text{ cm}^{-3}$ level and a slightly deeper level at $\sim 7\times 10^{14} \text{ cm}^{-3}$, which may be attributed to $EL15$.²⁷ It is noted that the n -type conductivity of the sample is attributed to these shallow levels since the presence of the deep donors $EL6$ and $EL2$ (present at the $7\times 10^{15} \text{ cm}^{-3}$ level) on their own would cause the sample to be semi-insulating. Further discussion of this data is given towards the end of the next subsection in the light of $EL6$ being DX -like and thus a double donor.

B. DLTS emission spectra

The DLTS signatures recorded (at $t_w = 13.6$ ms) for the trap filling times of 10-ns, 10- μs , and 100-ms durations are shown in Figs. 2(a), 2(b), and 2(c), respectively, for the $EL6$ peak. As observed by others,^{1–3} a distinguishing feature of the $EL6$ peak is noted, namely, that it is accompanied by small unresolved peaks (shoulders) on either side of it. By resolving the two shoulder peaks from $EL6$, through a non-linear curve fitting program, the activation energies were measured to be 0.28 ± 0.01 eV for the left shoulder peak and 0.40 ± 0.01 eV for right shoulder peak, which allowed their identification with the $EL7$ and $EL5$ levels, respectively.²⁷ For short filling times of nanoseconds duration, $EL7$ and $EL6$ peaks are observed, with the former appearing at slightly higher concentration. For filling pulses in the micro-seconds range, the defect concentration of the $EL6$ level is seen to rise above the $EL7$ level by about a factor of 3. For the still longer filling pulses (in the seconds range), $EL5$

begins to increase with a correlated reduction of the $EL6$ level intensity. This latter transition $EL6\rightarrow EL5$ has been documented recently by Shiraki, Tokuda, and Sassa,³⁰ but it appears that these workers did not use filling times short enough to see the faster $EL7\rightarrow EL6$ transition.

To obtain more detailed information of the $EL5$, $EL6$, and $EL7$ defect families we have fitted the more exact form of emission DLTS spectrum as given by

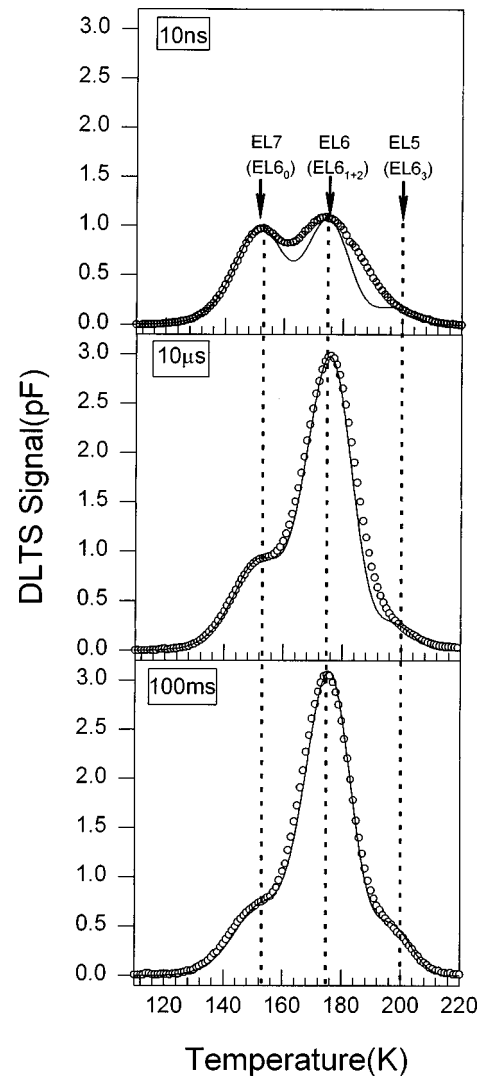


FIG. 2. DLTS emission spectra taken at trap filling times of 10 ns, 10 μs , and 100 ms and at a rate window time constant of 13.6 ms. The $EL6_0$ ($EL7$), $EL6_{1+2}$ ($EL6$), and $EL6_3$ ($EL5$) sublevels of the $EL6$ family referred to in the text are labeled. The solid lines correspond to the fitting of Eq. (3) to the data.

$$S(T) = C(t_1) - C(t_2) = C_0 \left[\left(1 + \sum_i \frac{N_{Ti}}{N_D} [1 - e^{-e_{ni}t_1}] \right)^{1/2} - \left(1 + \sum_i \frac{N_{Ti}}{N_D} [1 - e^{-e_{ni}t_2}] \right)^{1/2} \right], \quad (3)$$

which remains valid under the prevailing condition $N_D \sim N_T$. Here C_0 is the capacitance at the instant of reverse bias, t_1 and t_2 are the sampling times of the capacitance transient, N_{Ti} is the amount of the i th EL6 sublevel formed during trap filling, and e_{ni} is the trap emission rate at temperature T given by the standard expression²⁹

$$e_{ni} = N_C \sigma_i v_{th} \exp(-[E_C - E_i]/kT). \quad (4)$$

Here N_C is the effective density of states in the conduction band, v_{th} is the thermal carrier velocity, and σ_i and $E_C - E_i$ are the trap's capture cross section and energy level relative to the conduction band, respectively.

That we are in fact working in the regime where $N_D \sim N_T$ is confirmed in that if one tries to fit the shape of the DLTS spectra with the normally employed exponential approximation to Eq. (3) the fitting is found to be poor. The spectral shape, obtained using Eqs. (3) and (4), however, is good for the EL7 peak and reasonable for EL6. However, as can be seen in Fig. 2, the width of the measured EL6 peak is always noticeably larger than that predicted and it is thus possible that this peak is composed of two closely spaced peaks, in much the same way as that found for the central peak in the $\text{Al}_x\text{Ga}_{1-x}\text{As}:\text{Si}$ DX center spectrum.²³ In our spectra the EL5 peak was always present at too low a concentration to be able to make any deduction from its shape. In carrying out the fitting of Eqs. (3) and (4) the σ_i and $E_C - E_i$ are as determined from the standard Arrhenius DLTS plot and were thereafter kept fixed. In doing this we employ the fact that although the trap emission rate at the peak modal temperature does not correspond exactly to the rate window t_w defined conventionally as $(t_2 - t_1)/\ln(t_2/t_1)$ due to the form of Eq. (3), the structure of Eqs. (3) and (4) implies that $E_C - E_i$ can still be extracted correctly from the conventional plot of $\ln(t_w T^2)$ against $1/T$.

In view of the close connection seen in the present work between the satellite EL7 and EL5 levels and the EL6 level and the similarity between the spectral shape seen for the DX center in $\text{Al}_x\text{Ga}_{1-x}\text{As}:\text{Si}$,²³ the former two peaks are considered simply as sublevels of EL6 center in the remainder of the discussion. Moreover, in view of its width, the strong central peak is also considered to be composed of two close and difficult to separate sublevels. This is supported by the recent observation of Darmono *et al.*, who also attributed a wider than expected EL6-like peak in low-temperature grown GaAs to two closely spaced levels.³¹ To emphasize this multilevel structure of the same center and adopting the nomenclature of Su and Farmer,²³ we also refer to the EL7, EL6, and EL5 levels as $EL6_0$, $EL6_{1+2}$, and $EL6_3$, respectively. The intensities of the three resolved components relative to the background ionized donor concentration N_{Ti}/N_D were determined as parameters in the fitting of Eqs. (3) and (4). A small correction factor of magnitude $W_r^2/[W_r^2 - W_f^2]$ was then made to the N_{Ti}/N_D value to compensate for the fact that not all the traps in the depletion zone are under

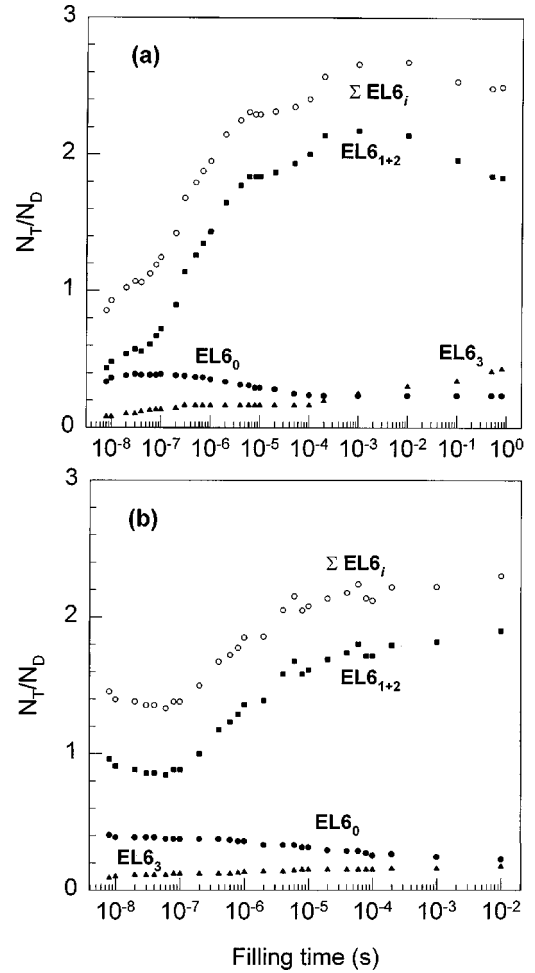


FIG. 3. Observed variation of the ‘‘relative to shallow donor’’ sublevel intensities N_{Ti}/N_D as a function of trap filling time for an emission time constant of (a) 13.6 ms and (b) 136 ms. The total relative to shallow donor EL6 concentration $\Sigma EL6_i$ is also shown.

emission, W_r and W_f being the depletion widths under reverse and forward biasing conditions.²⁹ The final ‘‘relative to shallow donor level’’ trap densities N_{Ti}/N_D are plotted in Figs. 3(a) and 3(b) for 13.6- and 136-ms emission rate-window time constants, respectively.

Clearly evidenced in Fig. 3 are the EL6 sublevel transformations $EL6_0 \rightarrow EL6_{1+2}$ and $EL6_{1+2} \rightarrow EL6_3$ that occur with increasing trap filling time. With specific reference to the 13.6-ms emission time constant data [Fig. 3(a)], it can be seen that the sublevel $EL6_0$ begins to increase up to trap filling times of ~ 30 ns and then starts decreasing in an approximately logarithmic form for longer filling pulses of millisecond duration. As the $EL6_0$ level drops, the $EL6_{1+2}$ level is seen to rise in a complimentary logarithmic fashion, reaching a maximum at filling times of ~ 1 ms. For filling times in excess of 1 ms the $EL6_{1+2}$ level begins to fall and over this same filling time range (1 ms to 1 s) the $EL6_3$ sublevel intensity increases slowly. Experimental limitations restricting the filling pulse time to less than 1 s meant that the evolution of the $EL6_3$ and the associated changes in the $EL6_0$ and $EL6_{1+2}$ sublevels could not be studied in any detail. Another experimental limitation is seen at the shorter filling times (less than ~ 100 ns), where, similar to the data of Su and Farmer,²³ one would expect the sublevel intensities

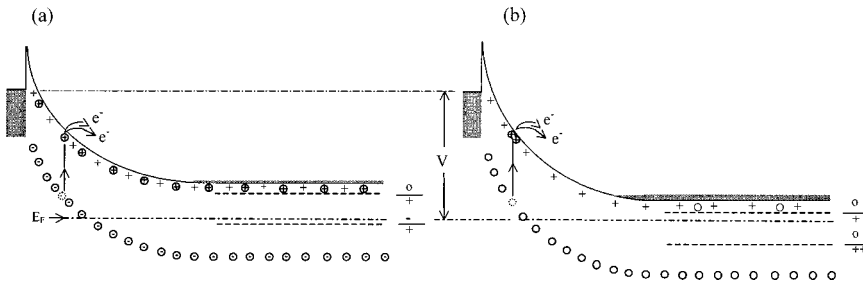


FIG. 4. Band bending diagrams at the instant of reverse bias V for the $EL6$ trap having charge states (a) $-/0/+$ and (b) $0/+$.

to approach zero as the filling pulse width is reduced. Instead, Fig. 3 shows the $EL6_0$ and $EL6_{1+2}$ sublevel intensities saturating in this time regime. This results from the fact that our apparatus has a total trap emission time not much longer than the second capacitance sampling time t_2 .²⁵ As a result, some fraction of the $EL6$ traps never fully ionize and a quiescent level of traps always remain in the electron occupied state.

As argued by Su and Farmer,²³ the observed behavior of sublevel transformations as seen in Fig. 3 can only be readily explained if the $EL6$ defect is DX -like in nature. This follows because a DX center not only has the capacity to donate a single electron to produce an ionized state, but in addition has the capability of recapturing two electrons in negative- U ordering to form the system's ground state. This is nicely expressed through the trapping rate c_{ni} into a site i of the defect for the negative- U two-electron capture process, which is given by²⁵

$$c_{ni} = C \exp\left(-\frac{E_{\text{cap}}}{kT}\right) n_C^2 (2N_i - n_i), \quad (5)$$

where E_{cap} is the capture activation energy, n_C is the free carrier density, N_i are the number of defect sites of type i , and n_i is electron occupancy of the site. From Eq. (5) it is noted that each site has the capacity to receive two electrons ($n_i = 2N_i$) and until this situation is obtained, some empty trap sites will be available to capture those electrons that have been emitted from other traps. It is this capacity for capturing two electrons that is of importance because, unlike the case of a single-occupancy center in which the system ground state is that of one electron trapped per center, the system's ground state is with two electrons on every other center. In other words, at least half of the centers will be in the fully ionized state. It is this fact that makes charge redistribution possible since, if a pair of electrons is thermally emitted from an $EL6$ center into the conduction band, then there are still a large number of unoccupied deep $EL6$ states available for recapturing the electrons. With emission being faster for the shallower sublevels through the $E_C - E_i$ dependence in Eq. (4), the electrons from the shallower states tend to redistribute to the deeper-lying states, thus explaining the direction of the $EL6_0 \rightarrow EL6_{1+2} \rightarrow EL6_3$ transformation with the increasing filling pulse duration. The result is a complex nonexponential time-dependent sublevel repopulation referred to as charge redistribution.²³ In the present context, however, it is noted that while this picture may hold exactly for the case of $Al_xGa_{1-x}As:Si$, where each Si center donates an electron and may receive two, the same ideality is not expected in the present case where an independent shallow donor forms an additional supply of electrons. We dis-

cuss this point further below, where it is suggested that charge redistribution still occurs because the concentration of the shallow donor state ($\sim 7 \times 10^{14} \text{ cm}^{-3}$) is significantly less than that of the $EL6$ state [$\sim (1.5-3) \times 10^{15} \text{ cm}^{-3}$].

If the above processes are correct, then it follows that charge redistribution between the different $EL6$ sublevels should take place only on a time scale commensurate with the emission time scales. A quick look at Fig. 3 shows that this prediction is indeed borne out. For the data in Fig. 3(a), which are taken with a relatively short emission rate (13.6 ms) (temperature of sample ~ 160 K), the data show clearly that redistribution under capture conditions is occurring over this time scale. However, on cooling the sample to 140 K the $EL6$ emission rate has decreased to 136 ms and charge redistribution is not so noticeable [Fig. 3(b)].

It is of interest to consider the charge states of the $EL6$ center. We consider two possibilities. The first is that it could have the charge states $-/0/+$ in likeness to the DX center in $Al_xGa_{1-x}As:Si$. The alternative is that it could have the charge states of the negative- U ordered Si vacancy, namely, $0/+/+$.³² We shall argue that the evidence favors the latter, although experimental uncertainty means that the former cannot be totally ruled out. A comparison of these two schemes may be made with reference to Fig. 4, where the band bending expected for both situations is portrayed at the instant of applying reverse bias V . In Fig. 4(a) the $-/0/+$ scheme is represented for the case of $N_6 > N_D$, which is suggested from Table I [$N_6 = (2.7 \pm 0.2) \times 10^{15} \text{ cm}^{-3}$, $N_D = (1.0 \pm 0.3) \times 10^{15} \text{ cm}^{-3}$]. Under these conditions it is expected that the deeper DX state will pull the Fermi energy down to the $+/-$ occupancy level, which, taking the activation energy of the $EL6$ center as 0.4 eV, will lie approximately 0.2 eV below the conduction band. The free-electron concentration n_C will be significantly smaller than N_D due to the compensation of the $EL6^-$ states by the $EL6^+$ states. The problems associated with this scheme are twofold. The first is that the exposed charge on reverse bias $\sim n_C$ is too small to account for the observed capacitance at the instant of reverse bias ($C_0 = 12$ pF). The second is that the relative to shallow donor DLTS signal amplitude (N_T/N_D) will be of magnitude $\sim 2N_6/n_C \gg 2N_6/N_D = 5.4 \pm 0.4$ and thus would be much larger than the observed value, which as seen from Fig. 3 is ~ 2.5 . From these considerations it may be concluded that if the $EL6$ center is indeed of $-/0/+$ character then it must be that $N_6 < N_D$ and some significant systematic error has occurred in the $C-V$ measurement of $N_6 + N_D$. Assuming that this is the case, the majority of $EL6$ will be in their negative state and instantaneous exposed charge on biasing is $N_D - N_6 \sim N_D$. With N_6 only fractionally lower than N_D , it would then be possible to get a reasonable value for

the instantaneous reverse capacitance and an N_T/N_D [$\approx 2N_6/(N_D - N_6)$] close to the observed value of ~ 2.5 .

Considering now the $0/+//+$ scheme, which is shown in Fig. 4(b), one notes that due to the double charging on each ionized center, the observed N_T from the C - V analysis is not N_6 but $2N_6$. Thus, from Table I one has $N_6 = (1.3 \pm 0.2) \times 10^{15} \text{ cm}^{-3}$. The instantaneous exposed charge being $N_D \approx 1 \times 10^{15} \text{ cm}^{-3}$ gives a reasonable C_0 value and the N_T/N_D value is simply $2N_6/N_D = 2.7 \pm 0.8$, which is in reasonable agreement with experiment. The $0/+//+$ scheme thus appears to be the more favored of the two. In the $-/0/+$ scheme [Fig. 4(a)], however, the charge redistribution phenomenon would be a natural consequence of approximately half of the $EL6$ centers being in the negative state under charge neutral conditions. As with the DX center in $\text{Al}_x\text{Ga}_{1-x}\text{As}:\text{Si}$ during pulse filling, it can never arise that more than half of the centers are occupied and thus there would always be states available for reemitted electrons. On the other hand, the more likely $0/+//+$ charge state scheme presents a problem for charge redistribution in this respect. Here the stable charge state of the $EL6$ center in the neutral bulk is dominantly the fully two electron occupied $EL6^0$, thus providing no unfilled states to facilitate charge redistribution. The answer as to why the charge redistribution phenomenon is observed is thus not immediately clear. It is noted, however, that during the initial stages of trap filling the density of electrons is only $\sim N_D$ and remains at this level for some time because of the tendency for the Fermi level to be pinned around the $0/+//+$ occupancy level. A large fraction of non-neutralized $EL6^{++}$ centers would thus persist, allowing some observed charge redistribution.

There is presently no firm consensus on the microstructure of the $EL6$ center. Some of the models that have been proposed are the complex defects $V_{\text{Ga}}\text{-As}_i$,^{31,33} $V_{\text{As}}\text{-As}_i$,^{27,34} and the divacancy $V_{\text{As}}\text{-V}_{\text{Ga}}$ possibly associated with As_i .^{3,4} It is natural to ask whether the observed DX -like nature of the $EL6$ family of levels can reveal any important information that might be helpful in determining the microstructure of the defect center. The likeness of the $EL6$ spectral features and their unusual filling pulse dependence closely resemble those arising from the DX center in $\text{Al}_x\text{Ga}_{1-x}\text{As}:\text{Si}$ have already been noted. This suggests that in looking at various candidates for the $EL6$ microstructure, the basic vacancy-interstitial model that applies to both Si- and Sn-doped $\text{Al}_x\text{Ga}_{1-x}\text{As}$ (Refs. 35–38) should be considered first in preference to more complex schemes. The $V_{\text{Ga}}\text{-As}_i$ and $V_{\text{As}}\text{-As}_i$ microstructures would thus be favored in which an As atom after a double electron capture moves, as a result of bond breaking, from its original lattice site towards any one of four ($i=0-3$) slightly different threefold coordinated interstitial sites. Since in the $V_{\text{As}}\text{-As}_i$ case such spontaneous bond breaking would require energy, the presence of a third component, however, must be postulated that would suggest models such as $(V_{\text{As}}\text{-V}_{\text{Ga}})\text{-As}_i$, $\text{As}_{\text{Ga}}\text{-V}_{\text{As}}\text{-As}_i$, or $\text{As}_{\text{Ga}}\text{-V}_{\text{Ga}}\text{-As}_i$. Other evidence for such a three-bodied structure comes from the observed hopping-type conduction in boron-implanted GaAs, which suggests some interaction between the As_{Ga} antisite defect $EL2$ and the $EL6$ center.³⁹ Site symmetry information on these two defects obtained from uniaxial stress measurements is supportive of such a view.¹¹ Such a close interaction between the two most domi-

nant native defects in GaAs suggests some physical proximity in the form of an associate complex such as $\text{As}_{\text{Ga}}\text{-V}_{\text{As}}(\text{V}_{\text{Ga}})\text{-As}_i$ involving the As_{Ga} antisite.⁴⁰ On the other hand, the simplicity of the $V_{\text{Ga}}\text{-As}_i$ model is attractive since the substitutional configuration is the As_{Ga} antisite and would thus be closely linked with $EL2$. Such hypotheses and arguments are at the present time necessarily speculative and indicate a need for a much closer study of the DLTS spectral fine structure coupled with detailed theoretical calculations of the energy states of various possible structures.

C. DLTS capture spectra

It is well established that the physical mechanism behind the observation of PPC in III-V materials in the presence of a large capture barrier between the excited charge carrier (in the conduction band) and the defect center.¹⁸ In other words, the photoexcited defect has to overcome a large barrier before being able to return to its ground state after illumination has stopped. The formation of such a barrier is a result of the large lattice relaxation that the defect center undergoes after photoionization. Thus one of the necessary conditions to classify a deep level as DX -like is to show that its photoexcited state possesses a capture barrier much larger than that expected for a simple atomic defect. This is clearly demonstrated by looking at the case of the $EL3$ defect, for which local vibrational mode measurements in SI GaAs reveal a double electron capture with negative- U ordering,⁴¹ but LLR (and thus by inference PPC) are apparently absent.¹²

The capture barrier E_B is generally expressed as

$$\sigma(T) = \sigma_\infty \exp\left(\frac{-E_B}{kT}\right), \quad (6)$$

where σ_∞ is the cross section for capture at an infinite temperature. The capture barrier is usually determined by measuring the temperature dependence of the cross section and thus by plotting the cross section against temperature a slope with gradient E_B is obtained. This method is costly in experimental time and prone to many systematic errors, such as filling pulse distortion by impedance mismatching between sample and pulse generator. Moreover, the normal saturation of defects during the filling pulse cycle is not found for the $EL6$ defect, making this approach difficult. This more straightforward and direct method employed by Ghosh and Kumar⁴² was thus adopted, which parallels closely the method for finding the trap activation energy in emission DLTS from the capacitance transient. In this method the rate window is opened on the capture capacitance transient rather than on the emission transient. The capture transient is of the form^{42,43}

$$C(t) = \sqrt{\frac{A^2 q \epsilon_s N_D}{V_{bi}}} \left(1 + \sum_i \frac{N_i}{N_D} \exp(-c_{ni}t) \right), \quad (7)$$

where c_{ni} , the capture rate into the trap giving the i th sub-level, is given by

$$c_{ni} = \sigma_\infty n \nu_{\text{th}} \exp\left(\frac{-E_B}{kT}\right). \quad (8)$$

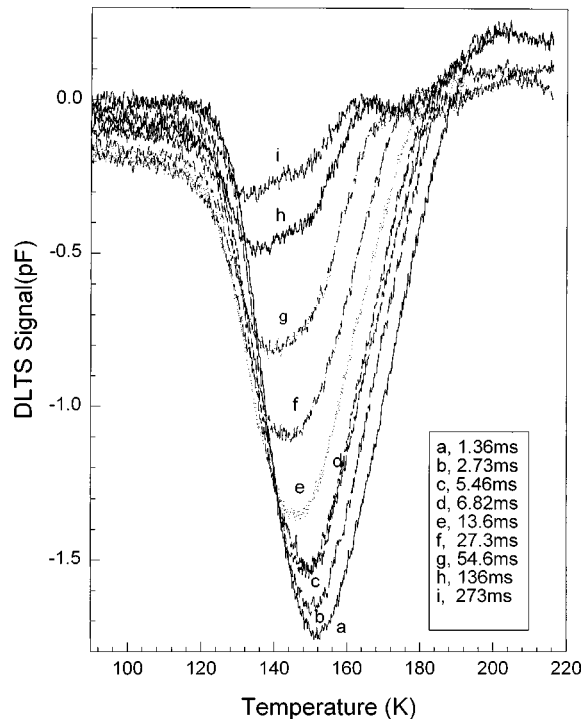


FIG. 5. DLTS capture spectra for the different rate capture windows indicated. The emission time was kept constant at 1 s.

As in emission DLTS, the spectrum $S(T)$ is given by $C(t_1) - C(t_2)$. The capture DLTS spectra recorded on the $EL6$ defect family for several rate windows and a trap emission time of 1 s are shown in Fig. 5. Two components, which are just resolvable through nonlinear curve fitting, are found to be present in these spectra. These are attributed to the $EL6_0$ and $EL6_{1+2}$ sublevels since by comparison the $EL6_3$ level seen under emission has a relatively small intensity.

Under our sample conditions, for which $N_D \sim N_i$, $S(T)$ takes on a mathematically complex shape similar to that obtained under emission as given in Eq. (3). We have not attempted a fitting of this form since, as with emission DLTS, the value of E_B from an Arrhenius plot of $\ln(t_w T^{1/2})$ versus $1/T$ may still be obtained (the $T^{1/2}$ factor coming from v_{th}) by taking T as the modal temperature of the sublevel peak and the rate window t_w defined conventionally. The Arrhenius plots corresponding to $EL6_0$ and $EL6_{1+2}$ are shown in Fig. 6, from which the capture barriers are determined to be 0.73 ± 0.1 and 0.6 ± 0.1 eV. These values are much greater than observed either for Si- or Sn-doped $Al_xGa_{1-x}As$, which have values of 0.2–0.36 eV (Refs. 42 and 44) and 0.11–0.15 eV,⁴⁵ respectively, or the value of 0.137 eV observed for the DX center in $Al_xAs_{1-x}Sb$.⁴³ While the large E_B values we find for $EL6$ are supportive of the LLR hypothesis, the excessively large value is cause for concern. It is not difficult, however, to find a reason for the value that we measure being too high. The suggestion has been made above that the Fermi energy, during the initial stages of trap filling, is pinned about the $+/++$ occupancy level until a significant fraction of the $EL6$ centers have ionized. Since the density of carriers n is expected to go as $\exp[-(E_C - E_{+/+})/kT]$ during the early stages of trap filling, it follows from Eq. (8) that the capture rate will vary according to $\exp[-(E_C - E_{+/+} + E_b)/kT]$. With this $E_C - E_{+/+}$ being ~ 0.4 eV for the $EL6$ center, E_b for

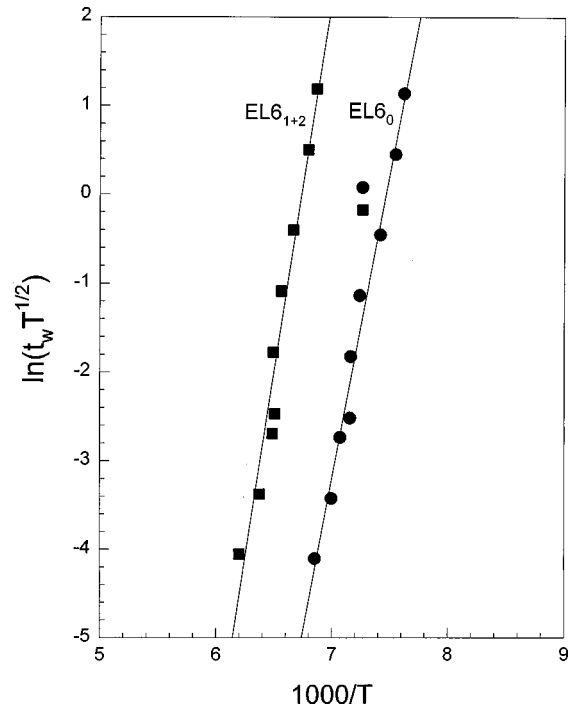


FIG. 6. Arrhenius plot $\ln(t_w T^{1/2})$ versus $1000/T$ for the two resolved capture DLTS sublevels $EL6_0$ and $EL6_{1+2}$. The gradients of the plots give energies of 0.59 ± 0.11 eV for $EL6_0$ and 0.79 ± 0.12 eV for $EL6_{1+2}$.

$EL6$ would thus lie in the more reasonable range 0.2–0.33 eV. Moreover, a capture barrier of this magnitude is quite consistent with the configuration coordinate diagram drawn by Chantre, Vincent, and Bois based on the optical absorption of $EL6$.¹⁰

IV. CONCLUSIONS

In carrying out conventional DLTS studies we have, as with many previous workers, observed a fine structure associated with the $EL6$ peak in n -type GaAs and have explained this structure in terms of similar, but not identical, possible ground-state relaxations of a certain native defect center. In addition, we have reported a charge redistribution between the various sublevels that occurs on filling the centers with electrons. Employing a direct comparison with the same fine structure and electron filling effects seen in $Al_xGa_{1-x}As:Si$, we have argued that these observations are firm evidence that $EL6$ is a DX -like center with a negative- U electron ordering. Although our data cannot with certainty distinguish the charge state of the $EL6$ ground state, which could either be negative or neutral, the evidence favors the latter. This would place the $EL6$ defect more in the category of a double donor having negative- U ordering, such as the monovacancy in silicon. It has been argued that in this case charge redistribution between the different ground-state relaxations is still possible because the Fermi energy is pinned around the $+/++$ level of the defect center for some time after commencement of filling. This pinning keeps the availability of conduction-band electrons low and the availability of unoccupied sublevels high, thus facilitating redistribution.

The present work is strongly supportive of a LLR being associated with the ground state of the $EL6$ structure. Evi-

dence comes both from the observed fine structure, in that its interpretation is in terms of bond-breaking relaxations to various ground-state configurations, and a magnitude of the barrier activation energy typical of LLR (0.2–0.3 eV). In this regard the present results do indirectly support the suggestion that EL6 is the center responsible for the observed PPC metastability observed in SI GaAs below ~ 40 K.¹⁶ Here the metastability would be caused by the emission barrier (~ 0.3 –0.4 eV). Optical pumping of electrons from the valence band and subsequent capture into the EL6 neutral ground state has the consequence of leaving the *p*-type GaAs with an excess of holes to compensate for residual shallow acceptors.¹⁶

We have discussed the alternative microstructures of the EL6 center in light of the DX-like character of the center, pointing out that a simple large lattice relaxation of some substitutional atomic position (excited state) to some interstitial-vacancy configuration (ground state) is indicated. We have argued that this behavior suggests that structures such as $(V_{As}-V_{Ga})-As_i$, $As_{Ga}-V_{As}(V_{Ga})-As_i$, or simply

$V_{Ga}-As_i$ are likely candidates. One thing is clear, however, and this is that the threefold to fourfold symmetry-breaking interaction observed in the fine structure clearly reveals some important information on the various relaxations available to the EL6 center and further experiment combined with theoretical modeling should thus help elucidate the structure. With regard to the need for better data, our present experiment has been deficient in two respects. First, there has been the restriction imposed on the maximum filling time and second there have been problems with short pulse trap filling times due to the restricted emission time. Further experiments could make use of the isothermal rate-window scanning DLTS method^{22,43} to avoid these deficiencies.

ACKNOWLEDGMENTS

The authors would like to thank the University Grants Committee of Hong Kong for funding this work. We would also like to thank M. Gong for helpful discussions.

-
- ¹H. Shiraki, Y. Tokuda, K. Sassa, and N. Toyama, *J. Appl. Phys.* **76**, 791 (1994).
²F. D. Auret, A. W. R. Leitch, and J. S. Vermaak, *J. Appl. Phys.* **59**, 158 (1986).
³Z.-Q. Fang, T. E. Schlesinger, and A. G. Milnes, *J. Appl. Phys.* **61**, 5047 (1987).
⁴C. V. Reddy, S. Fung, and C. D. Beling, *Phys. Rev. B* **54**, 11 290 (1996).
⁵H. J. von Bardeleben, D. Stiévenard, D. Deresmes, A. Huber, and J. C. Bourgoin, *Phys. Rev. B* **34**, 7192 (1986).
⁶W. Siegel, G. Kühnel, H. A. Schneider, H. Witte, and T. Flade, *J. Appl. Phys.* **69**, 2245 (1991).
⁷T. Hashizume and H. Nagabuchi, *Semicond. Sci. Technol.* **4**, 427 (1989).
⁸D. C. Look, P. W. Yu, W. M. Theis, W. Ford, G. Mathur, J. R. Sizelove, D. H. Lee, and S. S. Li, *Appl. Phys. Lett.* **49**, 1083 (1986).
⁹G. Kühnel and W. Siegel, *Semicond. Sci. Technol.* **6**, 1029 (1991).
¹⁰A. Chantre, G. Vincent, and D. Bois, *Phys. Rev. B* **23**, 5335 (1981).
¹¹M. Levinson, *Inst. Phys. Conf. Ser.* **91**, 73 (1987).
¹²C. A. Londos and T. Pavelka, *Semicond. Sci. Technol.* **5**, 1100 (1990).
¹³D. V. Lang and R. A. Logan, *Phys. Rev. Lett.* **39**, 635 (1977).
¹⁴J. Jiménez, P. Hernández, J. A. de Saja, and J. Bonnafé, *Phys. Rev. B* **35**, 3832 (1987).
¹⁵Yoh. Mita, *J. Appl. Phys.* **61**, 5325 (1987).
¹⁶W. C. Mitchel and J. Jiménez, *J. Appl. Phys.* **75**, 3060 (1994).
¹⁷D. J. Chadi and K. J. Chang, *Phys. Rev. Lett.* **61**, 873 (1988).
¹⁸P. M. Mooney, *J. Appl. Phys.* **67**, R1 (1990).
¹⁹S. Ghosh and V. Kumar, *J. Appl. Phys.* **46**, 7533 (1992).
²⁰M. O. Watanabe, K. Morizuka, M. Mashita, Y. Ashizawa, and Y. Zohta, *Jpn. J. Appl. Phys., Part 2* **23**, L103 (1984).
²¹H. P. Hjalmarson and T. J. Drumond, *Appl. Phys. Lett.* **48**, 656 (1986).
²²E. Calleja, F. Garcia, A. Gomez, E. Muñoz, P. M. Mooney, T. N. Morgan, and S. L. Wright, *Appl. Phys. Lett.* **56**, 934 (1989).
²³Z. Su and J. W. Farmer, *Appl. Phys. Lett.* **59**, 1746 (1991).
²⁴Z. Su and J. W. Farmer, *Appl. Phys. Lett.* **59**, 1362 (1991).
²⁵C. V. Reddy, S. Fung, and C. D. Beling, *Rev. Sci. Instrum.* **67**, 257 (1996).
²⁶C. V. Reddy, S. Fung, and C. D. Beling, *Rev. Sci. Instrum.* **67**, 4279 (1996).
²⁷G. M. Martin, A. Mitonneau, and A. Mircea, *Electron. Lett.* **13**, 191 (1977).
²⁸R. R. Senechal and J. Basinski, *J. Appl. Phys.* **39**, 3723 (1968).
²⁹J. Bourgoin and M. Lannoo, in *Point Defects in Semiconductors II*, edited by M. Cardona, P. Fulde, and H. J. Queisser, Springer Series in Solid-State Sciences Vol. 35 (Springer-Verlag, Berlin, 1983), Chap. 6.
³⁰H. Shiraki, Y. Tokuda, and K. Sassa, in *Defect- and Impurity-Engineered Semiconductors and Devices*, edited by S. Ashok, J. Chevallier, I. Akasaki, N. M. Johnson, and B. L. Soporó, MRS Symposia Proceedings No. 378 (Materials Research Society, Pittsburgh, 1995), p. 935.
³¹J. Darmo, F. Dubecký, P. Kordoš, and A. Förster, *Appl. Phys. Lett.* **72**, 590 (1998).
³²G. D. Watkins and J. R. Troxell, *Phys. Rev. Lett.* **44**, 593 (1980).
³³R. Yakimova, T. Paskova, and Ch. Hardalov, *J. Appl. Phys.* **74**, 6170 (1993).
³⁴D. Stiévenard, X. Boddaert, J. C. Bourgoin, and H. J. von Bardeleben, *Phys. Rev. B* **41**, 5271 (1990).
³⁵T. N. Morgan, *J. Electron. Mater.* **20**, 63 (1991).
³⁶U. Scherz and M. Scheffler, in *Semiconductors and Semimetals*, edited by R. K. Willardson and A. C. Beers (Academic, New York, 1993), Vol 38.
³⁷D. J. Chadi, *Phys. Rev. B* **46**, 6777 (1992).
³⁸J. Mäkinen, T. Laine, K. Saarinen, P. Hautojärvi, C. Corbel, V. M. Airaksinen, and P. Gibart, *Phys. Rev. Lett.* **71**, 3154 (1993).
³⁹P. Langlade and S. Makram-Ebeid, *Inst. Phys. Conf. Ser.* **74**, 281 (1985).
⁴⁰J. Samitier, J. R. Morante, L. Giraudet, and S. Gourrier, *Appl.*

- Phys. Lett. **48**, 1138 (1986).
- ⁴¹U. Kaufmann, E. Klausmann, J. Schneider, and H. Ch. Alt, Phys. Rev. B **43**, 12 106 (1991).
- ⁴²S. Ghosh and V. Kumar, J. Appl. Phys. **75**, 8243 (1994).
- ⁴³D. K. Johnstone, Y. K. Yeo, R. L. Hengehold, and G. W. Turner, Appl. Phys. Lett. **71**, 506 (1997).
- ⁴⁴N. S. Caswell, P. M. Mooney, S. L. Wright, and P. M. Solomon, Appl. Phys. Lett. **48**, 1093 (1986).
- ⁴⁵Q. S. Huang, H. Lin, J. Y. Kang, B. Liao, W. G. Tang, and Z. Y. Li, J. Appl. Phys. **71**, 5952 (1992).